Extension of the ITU Channel Models for Wideband (OFDM) Systems

Troels B. Sørensen, Preben E. Mogensen
Department of Communication Technology
Aalborg University
Niels Jernes Vej 12, DK9220 Aalborg, Denmark
{tbs, pm}@kom.aau.dk

Frank Frederiksen
Nokia Networks
Niels Jernes Vej 10, DK9220 Aalborg, Denmark
frank.frederiksen@nokia.com

***Abstract*— This paper outlines a procedure to extend, or upsample, the ITU *power delay profiles* (PDP) to improve the frequency correlation properties while keeping the same mean delay and almost the same rms delay spread. Realistic frequency correlation properties are of particular importance for the evaluation of wideband system concepts with frequency dependent characteristics, e.g. frequency domain link adaptation and packet scheduling, both of which are likely to be part of future wideband systems such as based on OFDM. With the suggested procedure the frequency correlation can be kept approximately at or below 0.6 for frequency separations up to 25 MHz for the exemplified ITU Vehicular A and Pedestrian B channel profiles. The compatibility in terms of link level performance with WCDMA rake processing and the representation of the profiles on different sampling grids is briefly discussed in the paper.**

ITU Channel models; frequency correlation function; wideband systems; power delay profile; beyond 3G system concepts

I. INTRODUCTION

The ITU power delay profiles defined by the recommendations of the ITU [1], including the Vehicular A (Veh. A) and Pedestrian B (Ped. B) primarily discussed in this paper, are well-established channel models for research of mobile communication systems. They specify channel conditions for various operating environments encountered in third-generation wireless systems, e.g the UMTS Terrestrial Radio Access System (UTRA) standardised by 3GPP. These systems operate in a 5 MHz bandwidth and are based on CDMA principles.

Due to this acceptance and familiarity it is of interest to base also future system studies on models which are compatible with, or can be referenced to, the original ITU models. However, for the investigation of OFDM based systems with larger operating bandwidths the models are less suitable as they show an apparent periodicity in their frequency correlation properties with high correlation levels for even large frequency separations - an artifact which is inconsistent with measured frequency correlations. This is believed to impact on the performance of OFDM based systems where typically frequency domain link adaptation and packet scheduling is applied. In this paper, we focus on system concepts for beyond 3G (B3G) communications with target operating bandwidths in the order of 20 MHz.

Later we define the *frequency correlation function* (FCF) which can be interpreted as the likelihood that two signals at a certain frequency separation will fade together. Although significant correlation between widely separated frequencies can occur there is no obvious reason why this should represent an average behaviour of the channel. While measured frequency correlations have not been studied extensively, there are references which show that the correlation decays steadily with increasing frequency separation. One example is from the HIPERLAN Medbo E model [2] which is applicable for outdoor large open spaces. This model is derived directly from wideband measurements (20 MHz) and show very low correlation levels (below 0.35) for frequency separations above 2 MHz. Another example measurement with higher overall correlation, but same steady decay, is mentioned in [3], and a more recent publication [4] including measurements in 100 MHz bandwidth from an urban area leads to the same conclusion.

It is not the purpose of this paper to provide empirical evidence, nor accurate modelling, of the frequency correlation. Rather, we start in Section II with a consideration of the frequency correlation properties of the ITU profiles, and then suggest a procedure in Section III to extend, or upsample, the profiles to improve the properties in the direction of the empirical observations. In Section IV we show the result of applying the procedure to two different ITU profiles and discuss the representation of the extended profiles on different sampling grids as well as their compatibility to the original profiles in terms of link level performance for WCDMA systems with rake receiver processing. Finally, we conclude in Section V.

II. THE ITU CHANNEL MODELS

The ITU profiles model the temporal dispersion of the time-variant wireless propagation channel, $h(\tau;t)$, as a discrete tapped-delay-line with K taps.

$$h(\tau;t) = \sum_{k=1}^{K} a_k^t \delta(\tau - \tau_k) \qquad (1)$$

The tapped-delay-line model represents a *wide sense stationary uncorrelated scattering* (WSSUS) channel [5] as long as the time-variant tap coefficients, a_k^t, are uncorrelated Gaussian random processes. In fact, all the ITU channel

models in [1] have *independent identically distributed* (*iid*) zero mean complex Gaussian tap amplitudes.

The auto-correlation function of $h(\tau;t)$ for the WSSUS channel is given by

$$\begin{aligned}\varphi_h(\tau_1;\tau_1;t_1;t_2) &= E\left[h(\tau_1;t_1)^* h(\tau_2;t_2)\right] \\ &= \varphi_h(\tau_1;\Delta t)\delta(\tau_1-\tau_2)\end{aligned} \quad (2)$$

and hence depends only on the time difference $\Delta t = t_2 - t_1$. From this we define the multi-path intensity profile $\varphi_h(\tau_1;0)$, or simply $\varphi_h(\tau)$, as the *power delay profile* (PDP). The stem plot in Fig. 1 shows the PDP for the ITU Veh. A channel profile with excess tap delay on the abscissa and relative normalised tap power ($\sum_k E\left[\left|a_k^t\right|^2\right] = 1$) on the ordinate.

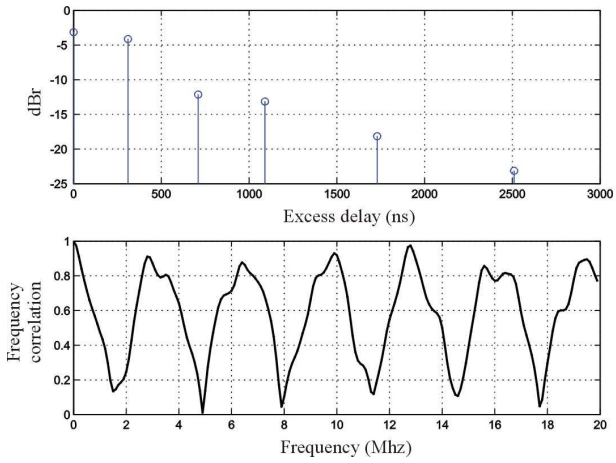

Figure 1. ITU Veh. A channel profile and its corresponding FCF. The profile has 6 channel taps with a *gcd* of 10 ns (see text), mean delay of 254 ns, and rms delay spread of 370 ns [1].

From $\varphi_h(\tau_1;\Delta t)$ we similarly define the spaced-frequency, Δf, spaced-time, Δt, correlation function

$$\begin{aligned}\varphi_H(\Delta f;\Delta t) &= E\left[H^*(f_1;t_1)H(f_1+\Delta f;t_1+\Delta t)\right] \\ &= \int_{-\infty}^{\infty}\varphi_h(\tau_1;\Delta t)e^{-j2\pi\Delta f\tau_1}d\tau\end{aligned} \quad (3)$$

where $H(f;t) = \int_{-\infty}^{\infty} h(\tau;t)e^{-j2\pi f\tau}d\tau$, defined as the Fourier transform of $h(\tau;t)$, is the time-variant transfer function in the frequency variable *f*. Given the properties of the ITU profiles, $H(f;t)$ is also a zero mean complex Gaussian random process in the frequency variable [5]. This leads to identical fading distributions in the sub-carrier channels of *multicarrier modulation* (MCM) based systems, e.g OFDM. Only with correlated paths, or 2 or more Rician fading paths, will there be different fading distributions between sub-carrier channels [6].

With $\Delta t = 0$ we get the relation

$$\varphi_H(\Delta f) = \int_{-\infty}^{\infty}\varphi_h(\tau)e^{-j2\pi\Delta f\tau_1}d\tau \quad (4)$$

and define $|\varphi_H(\Delta f)|$ as the FCF.

For a WSSUS channel with an exponentially decaying power delay profile, $\varphi_h(\tau) = \left(1/\tau_{rms}\right)e^{-\tau/\tau_{rms}}$, the FCF is $\varphi_H(\Delta f) = (1 + j2\pi\tau_{rms}\Delta f)^{-1}$, in which τ_{rms} directly characterises mean excess delay, rms delay spread, and coherence bandwidth Δf_c: At correlation, or coherence, level $c = 1/\sqrt{2}$ where $|\varphi_H(\Delta f_c)|/|\varphi_H(0)| = c$, the coherence bandwidth is $\Delta f_c = 1/2\pi\tau_{rms}$ - an often used measure of the coherence bandwidth of arbitrary PDP. In general, the coherence bandwidth for WSSUS channels is lower bounded by $\arccos(c)/2\pi\tau_{rms}$ [7] which is approx. 78.5% of Δf_c for the exponential profile at the coherence level quoted above.

The FCF for the Veh. A profile is shown in Fig. 1, with correlation level on the ordinate and frequency separation on the abcissa. We mentioned earlier the apparent periodicity of the FCF for the ITU profiles by which we refer to the multiple lobes versus frequency that are not directly related to the periodicity of the FCF but rather to the (limited) number of and relative spacing of channel taps. Strictly speaking, the FCF is periodic with 1/*gcd*, where *gcd* is the greatest common divisor of the tap spacings [3]. Typically, the *gcd* defines the sampling grid for simulation implementation; for the ITU Veh. A it is 10 ns corresponding to a FCF periodicity of 100 MHz.

As we will see later, similar FCF behaviour applies to the Ped. B profile, and also other ITU profiles and other commonly applied channel models, e.g. the discrete COST259 TU model specified in TR25.943 [8]. The COST259 TU model is an exponentially decaying PDP (as is the ITU Indoor B), which in [8] has been represented as a discrete tapped-delay-line with 20 taps. This model is a good example that despite "a large number of taps" [8] has been selected it does not necessarily ensure realistic frequency correlation properties (even in 5 MHz bandwidth).

One of the problems with the model FCF (Fig. 1) is to make sense of the aforementioned coherence bandwidth measure, Δf_c, e.g. what does it mean at coherence level 0.6? This in particular applies to the ITU Pedestrian A (Ped. A) which exhibits very high correlation (above approx. 0.8) and to some extent also for the Vehicular B (Veh. B). The coherence bandwidth defined on the Veh. B profile is far from expectation based on its rms delay spread, e.g. applying $\Delta f_c = 1/2\pi\tau_{rms}$ as an estimate, and far from the uncertainty bound for WSSUS channels.

In the following, we show that by inserting only a few additional taps to the ITU Veh. A and Ped. B channel models we can improve the situation to get frequency correlation properties in closer agreement with measured correlation. We have specifically emphasised the ITU Veh. A and Ped. B, but improvements can also be obtained with a few additional taps and same sampling grids for the Indoor A and Veh. B profiles. The Indoor B, however, is better represented based on the equivalent time-continuous exponential profile (e.g. using the

procedure in [8]) and as it was justified earlier an extension of the Ped. A does not make much sense altogether.

III. EXTENSION FOR WIDEBAND SYSTEMS

For extending the ITU profiles we have applied a procedure inspired by the derivation of the so-called modified ITU profiles [9]. The aim was to have a defined backward compatibility to the original profiles in the sense of meeting the same mean excess delay, same rms delay spread, and same coherence bandwidth defined on the lower frequency portion of the FCF. Applying the method in [9] based on the tap spacing of the original profile reduces the extended profile to the same tap power as in the original, and hence in the extension we maintain in some sense the same overall shape of the PDP.

The developed procedure, illustrated in Fig. 2, consists in a power redistribution between the existing and additional taps inserted to the profile. The figure shows the original profile with tap position(s) τ_i and tap power $P(\tau_i) = E\left[\left|a_i^t\right|^2\right]$, and a new channel tap added at excess delay τ_a with power $P(\tau_a)$; due to the insertion of this new tap the power assigned to the original (neighbouring) tap positions will change to $P'(\tau_i)$. To calculate this change, we define a support function $x_i(\tau)$ which is the weight that we need to apply in calculating the contribution of power that $P(\tau_a)$ gives to the original channel tap at τ_i. Similarly, a function can be defined for the contribution to the tap at τ_{i+1}.

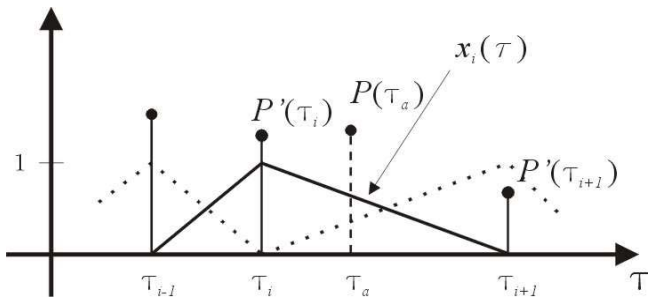

Figure 2. Power redistribution method.

$x_i(\tau)$ is defined by

$$x_i(\tau) = \begin{cases} \dfrac{\tau - \tau_{i-1}}{\tau_i - \tau_{i-1}}, & \tau_{i-1} < \tau < \tau_i \\ 1 - \dfrac{\tau - \tau_i}{\tau_{i+1} - \tau_i}, & \tau_i \le \tau < \tau_{i+1} \\ 0, \quad otherwise \end{cases} \tag{5}$$

From the definition of the weighting function it follows that if the original profile is normalised so is the extended (the procedure keeps the total power unchanged). Similar to the following derivation, it can be proved that with the assumption of a normalised profile, $\sum_k P(\tau_k) = 1$, the mean delay is unchanged after the insertion of the new tap; it can also be proved that this applies to repeated (nested) application of the procedure. Instead, to illustrate the basic procedure we can check the influence on the rms delay spread, or simply, with the same mean, the mean square delay $\overline{\tau^2}$ ($\tau_i \le \tau_a \le \tau_{i+1}$):

$$\begin{aligned} \overline{\tau^2} &= \sum_k \tau_k^2 P(\tau_k) = \sum_{k \notin \{i,i+1\}} \tau_k^2 P(\tau_k) + \\ &\tau_i^2 P'(\tau_i) + \tau_a^2 P(\tau_a) + \tau_{i+1}^2 P'(\tau_{i+1}) \\ &= \sum_{k \notin \{i,i+1\}} \tau_k^2 P(\tau_k) \\ &+\tau_i^2 \left(P(\tau_i) - x_i(\tau_a) P(\tau_a)\right) + \tau_a^2 P(\tau_a) \\ &+\tau_{i+1}^2 \left(P(\tau_{i+1}) - (1 - x_i(\tau_a)) P(\tau_a)\right) \\ &= \sum_k \tau_k^2 P(\tau_k) \\ &+P(\tau_a)\left(x_i(\tau_a)\left(\tau_{i+1}^2 - \tau_i^2\right) + \left(\tau_a^2 - \tau_{i+1}^2\right)\right) \end{aligned} \tag{6}$$

To evaluate any change to rms delay spread it suffices to consider only the term inside brackets in the last expression. Elaborating further we get

$$\begin{aligned} &\left(x_i(\tau_a)\left(\tau_{i+1}^2 - \tau_i^2\right) + \left(\tau_a^2 - \tau_{i+1}^2\right)\right) \\ &= \left(1 - \frac{\tau_a - \tau_i}{\tau_{i+1} - \tau_i}\right)(\tau_{i+1} - \tau_i)(\tau_{i+1} + \tau_i) \\ &+\left(\tau_a^2 - \tau_{i+1}^2\right) \\ &= -\tau_a(\tau_i + \tau_{i+1}) + \tau_i \tau_{i+1} + \tau_a^2 \\ &= \tau_a^2 - 2A\tau_a + G^2 \end{aligned} \tag{7}$$

where A is the arithmetic mean of τ_i and τ_{i+1}, $(\tau_i + \tau_{i+1})/2$, and G is the geometric mean, $\sqrt{\tau_i \tau_{i+1}}$. The last expression is that of a parabola with its vertex at A in which the value of the expression is $\left(G^2 - A^2\right)$, and zero intersections at $\tau_a = \{\tau_i, \tau_{i+1}\}$. Since from calculus $G \le A$, and in this case strictly less since $\tau_i \ne \tau_{i+1}$, delay spread will always decrease when applying the procedure. This also shows that there is no solution, in this formulation, to the more general problem of simultaneously optimising for tap delay and power under the constraint of same mean and same rms delay spread.

As it turns out, however, repeated application of the procedure can give quite reasonable frequency correlation properties for only a modest change in delay spread. The procedure was applied by inserting one tap at a time, with fixed constraints on the amount of power the new tap "contributes" to the neighbouring taps, either left or right, while at the same time observing the "evolution" of the frequency correlation as the tap position changes. Considerable heuristics was applied to find best compromises, e.g. for both Veh. A and Ped. B the best result is obtained by first inserting a new tap in the first interval (interval between the two leading taps of the original profile), followed by a tap in the second interval, and then finally again one in the first interval, in each case contributing about half the power of the neighbouring taps. For Veh. A, the delay spread decreases by approximately 3.5%, and no more than 1% for Pedestrian B.

IV. EXTENDED ITU MODELS

The resulting PDP and its corresponding FCF for the ITU Veh. A channel profile is shown in Fig. 3. We see that the frequency correlation has reduced from a maximum of approx. 1to 0.6 over a 20 MHz bandwidth (actually, this improvement is noticeable up to 25 MHz bandwidth). In Fig. 3 we have further imposed the constraint of having a *gcd* equal to 10 ns, and thereby represented on a sampling grid similar to the original Veh. A.

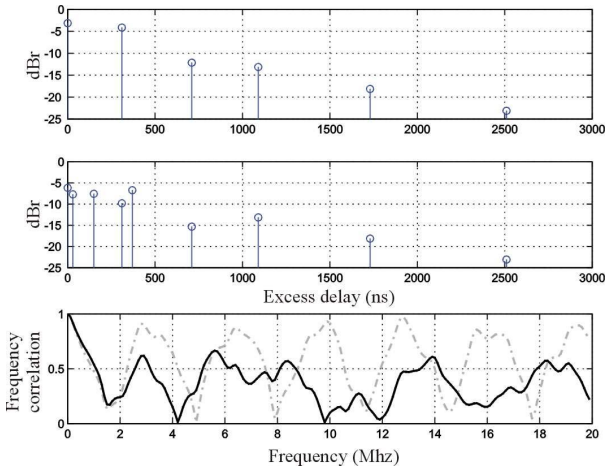

Figure 3. Original (top) and extended (centre) ITU Veh. A channel profile on a 10 ns sampling grid, and the comparison between their corresponding FCF (bottom). Tabulated values are given in the annex.

Further improvement with the method outlined in Section III is not straightforward, and especially the improvement from inserting additional taps does not pay off compared to the increased computational complexity with increasing number of taps. Also, we believe that the model in Fig. 3 has just acceptable frequency correlation properties for the study of wideband frequency dependent system concepts. A much similar improvement can be obtained for Ped. B as it is shown in Fig. 4.

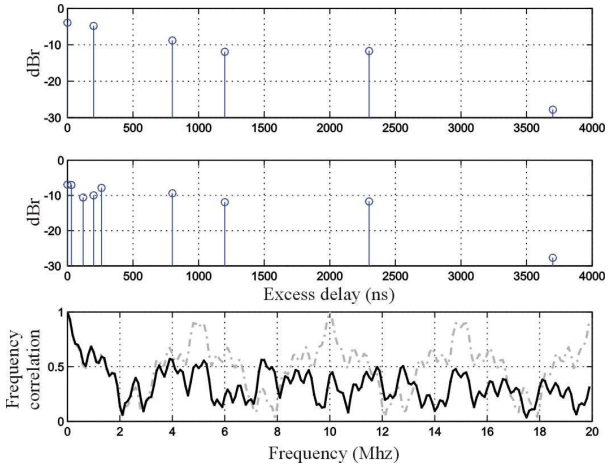

Figure 4. Same as Fig. 3, but for the ITU Ped. B channel profile. Tabulated values are given in the annex. The Ped. B profile has 6 channel taps with a *gcd* of 100 ns, mean delay of 409 ns, and rms delay spread of 633 ns [1].

With some increase of the correlation level, the procedure can be applied to represent the extended profile on other sampling grids to match specific simulation implementations. For aligning the profiles, besides the procedure leading to the modified ITU, a more commonly used method is coarse alignment where taps are combined on nearest grid points. To illustrate this representation for the previous two profiles consider the sampling rate of 30.72 MHz envisaged for the evolved UTRA radio-access concept [10], which defines a 32.55 ns sampling grid.

With this new grid, or constraint on the tap positions, we ran the procedure in Section III to redistribute power between the low excess delay taps, and applied coarse alignment of the remaining taps of the ITU profiles. The respective results can be seen in Fig. 5 and 6. The resulting FCFs are different, but exhibit almost the same overall improvement.

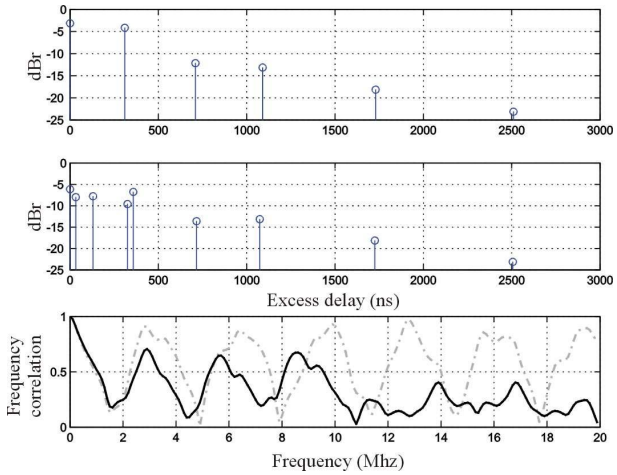

Figure 5. Original (top) and extended (centre) ITU Veh. A channel profile on a 32.55 ns sampling grid, and the comparison between their corresponding FCF (bottom). Tabulated values are given in the annex.

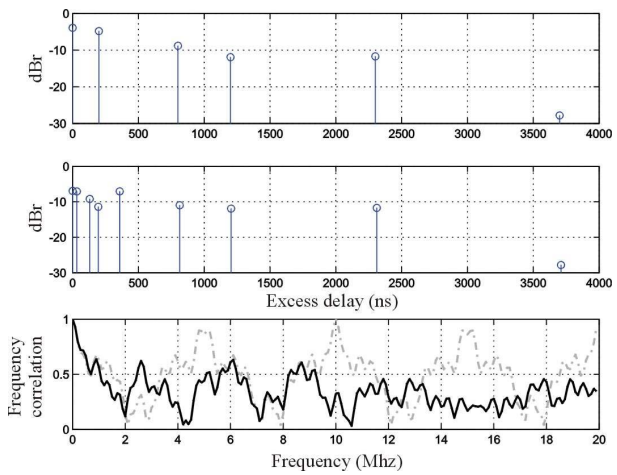

Figure 6. Original (top) and extended (centre) ITU Ped. B channel profile on a 32.55 ns sampling grid, and the comparison between their corresponding FCF (bottom). Tabulated values are given in the annex.

Apart from the legacy to well-known channel models, one other objective in using the ITU models as a basis was to

proliferate on the vast amount of reference results for WCDMA; such capability is desirable in the assessment and validation of performance for systems being designed for future systems. Due to the increase in the number of taps there is however significant performance degradation with WCDMA rake receiver processing when operating at high G-factors, that is, close to the base station; the additional taps lead to increased inter-path interference. In fact, calculating the orthogonality factor [11] for the original and extended Veh. A profile (10 ns grid) gives respectively 0.54 and 0.24, and thus illustrates a considerable loss of code orthogonality. This tells us that straightforward comparisons to previously obtained WCDMA results will be difficult.

V. CONCLUSION

This paper has explained and demonstrated a simple procedure for extending the well-established ITU power delay profiles to bandwidths exceeding their original 5 MHz target bandwidth. With the extension, it is possible to evaluate the performance of future wideband system concepts using bandwidths in excess of 20 MHz; at such bandwidths the extended models have frequency correlation properties which are clearly more realistic than the original models. This is of particular importance for systems with frequency dependent system characteristics, e.g. frequency domain link adaptation and packet scheduling.

With an increase of the number of channel taps from 6 to 9, it has been possible to improve the frequency correlation properties of the exemplified ITU Veh. A and Ped. B channel profiles. The extended profiles are backward compatible to the original profiles in the sense of meeting the same mean delay, same coherence bandwidth, and almost the same rms delay spread. They are represented on a 10 ns sampling grid similar to the original Veh. A profile and can be used for system bandwidths up to 25 MHz; over this bandwidth the frequency correlation stays at or below 0.6. Other sampling grids are also possible with almost the same overall performance.

REFERENCES

[1] "Guidelines for the evaluation of radio transmission technologies for IMT-2000," Recommendation ITU-R M.1225, 1997.

[2] J. Medbo and P. Schramm, "Channel models for HIPERLAN/2 in different indoor scenarios," ETSI BRAN 3ERI085B, March 1998.

[3] M. Pätzold, A. Szczepanski, and N. Youssef, "Methods for modelling of specified and measured multipath power-delay profiles," IEEE Trans. Veh. Techn., vol. 51, no. 5, September 2002.

[4] M. Riback, H. Asplund, J. Medbo, and J.-E. Berg, "Statistical Analysis of Measured Radio Channels for Future Generation Mobile Communication Systems," Proceedings of 61st IEEE Vehicular Technology Conference (VTC), Stockholm Sweden, May 2005.

[5] J. G. Proakis, Digital Communications, New York, John Wiley & Sons, 1987.

[6] K. Zhang, Z. Song, and L. Guan, "Multicarrier channels with non-identical subcarrier fading distributions – analysis and adaptation," IEEE Comm. Lett., vol. 8, no. 6, June 2004, pp. 368-370.

[7] B. H. Fleury, "An Uncertainty Relation for WSS Processes and Its Application to WSSUS Systems," IEEE Transactions on Communications, vol. 44, no. 12, December 1996, pp. 1632-1634.

[8] "Deployment aspects," Technical report 3GPP TR 25.943, v. 5.1.0 (2002-06), Technical Specification Group Radio Access Networks (Release 5).

[9] "Recommended simulation parameters for tx diversity simulations," 3GPP TSG RAN WG1 (TSGR1#14(00)0867), July 4-7, 2000, Oulu Finland.

[10] "Principles for the Evolved UTRA radio-access concept," 3GPP TSG RAN WG1 (R1-050622), June 20-21, 2005, Sophia Antipolis, France.

[11] C. Passerini and G. Falciasecca, "Correlation between delay-spread and orthogonality factor in urban environments," IEE Electronics Letters, vol. 37, no. 6, March 2001, pp. 384-386.

ANNEX

Table 1 Tabulated values for the extended ITU Veh. A. on 10 ns grid.

Excess tap delay (ns)	Relative power (dB) org. Veh. A	Relative power (dB) ext. Veh. A
0	0.0	0.00
30		-1.54
150		-1.40
310	-1.0	-3.64
370		-0.58
710	-9.0	-9.15
1090	-10.0	-6.97
1730	-15.0	-11.98
2510	-20.0	-16.93

Table 2 Tabulated values for the extended ITU Ped. B. on 10 ns grid.

Excess tap delay (ns)	Relative power (dB) org. Ped. B	Relative power (dB) ext. Ped. B
0	0.0	0.0
30		-0.1
120		-3.7
200	-0.9	-3.0
260		-0.9
800	-4.9	-2.5
1200	-8.0	-5.0
2300	-7.8	-4.8
3700	-23.9	-20.9

Table 3 Tabulated values for the extended ITU Veh. A and Ped. B. on a 32.55 ns sampling grid.

Excess tap delay (x 32.55 ns)	Relative power (dB) ext. Veh. A	Relative power (dB) ext. Ped. B
0	0.00	0.00
1	-1.85	-0.17
4	-1.64	-2.26
6		-4.48
10	-3.45	
11	-0.61	-0.14
22	-7.46	
25		-4.06
33	-6.99	
37		-4.99
53	-11.99	
71		-4.79
77	-16.99	
114		-20.89